

Asymmetries in the Production of Λ^0 in 250 GeV/c π^\pm , K^\pm and p – Nucleon Interactions

G.A. Alves,⁽¹⁾ S. Amato,^{(1), a} J.C. Anjos,⁽¹⁾ J.A. Appel,⁽²⁾ J. Astorga,⁽⁵⁾
 T. Bernard,^{(5), b} S.B. Bracker,^{(4), c} L.M. Cremaldi,⁽³⁾ W.D. Dagenhart,^{(5) d}
 C.L. Darling,⁽⁸⁾ D. Errede,^{(7), e} H.C. Fenker,^{(2), f} C. Gay,^{(4), g} D.R. Green,⁽²⁾
 R. Jedicke,^{(4), h} P.E. Karchin,⁽⁶⁾ S. Kwan,⁽²⁾ L.H. Lueking,⁽²⁾
 J.R.T. de Mello Neto,^{(1), a} J. Metheny,⁽⁵⁾ R.H. Milburn,⁽⁵⁾
 J.M. de Miranda,⁽¹⁾ H. da Motta,⁽¹⁾ A. Napier,⁽⁵⁾ M.S. Nicola,⁽¹⁾
 D. Passmore,⁽⁵⁾ A. Rafatian,⁽³⁾ A.C. dos Reis,⁽¹⁾ W.R. Ross,⁽⁸⁾
 A.F.S. Santoro,^{(1), i} M. Sheaff,⁽⁷⁾ M.H.G. Souza,⁽¹⁾ C. Stoughton,⁽²⁾
 M.E. Streetman,^{(2), c} D.J. Summers,⁽³⁾ S.F. Takach,⁽⁶⁾ A. Wallace,⁽⁸⁾ Z. Wu⁽⁸⁾

⁽¹⁾Centro Brasileiro de Pesquisas Físicas, Rio de Janeiro, Brazil

⁽²⁾Fermi National Accelerator Laboratory, Batavia, Illinois, 60510

⁽³⁾University of Mississippi, University, MS 38677

⁽⁴⁾University of Toronto, Toronto, Ontario, Canada, M5S 1A7

⁽⁵⁾Tufts University, Medford, MA 02155

⁽⁶⁾Wayne State University, Detroit, Michigan 48202

⁽⁷⁾University of Wisconsin, Madison, WI 53706

⁽⁸⁾Yale University, New Haven, CT 06511

(Fermilab E769 Collaboration)

^a Now at Universidade Federal do Rio de Janeiro, Rio de Janeiro, Brazil

^b Deceased

^c Retired

^d Now at Brandeis University, Waltham, MA 02454

^e Now at University of Illinois, Urbana, IL 61801

^f Now at Thomas Jefferson National Accelerator Facility, Newport News, VA 23606

^g Now at Yale University, New Haven, CT 06511

^h Now at LPL, University of Arizona, Tucson, AZ 85721

ⁱ Now at Universidade do Estado do Rio de Janeiro, Rio de Janeiro, Brazil

Abstract

Using data from Fermilab fixed-target experiment E769, we have measured particle-antiparticle production asymmetries for Λ^0 hyperons in 250 GeV/c π^\pm , K^\pm and p – nucleon interactions. The asymmetries are measured as functions of Feynman-x (x_F) and p_T^2 over the ranges $-0.12 \leq x_F \leq 0.12$ and $0 \leq p_T^2 \leq 3(\text{GeV}/c)^2$ (for positive beam) and $-0.12 \leq x_F \leq 0.4$ and $0 \leq p_T^2 \leq 10(\text{GeV}/c)^2$ (for negative beam). We find substantial asymmetries, even at x_F around zero. We also observe leading-particle-type asymmetries. These latter effects are qualitatively as expected from valence-quark content of the target and variety of projectiles studied.

Leading particle production effects have been studied both experimentally [1–6] and theoretically [7–11]. These effects are manifest as an enhancement in the production rate of particles that share one or more valence quarks with an initial state hadron compared to their antiparticles when they share either none or fewer. This enhancement is expected to become larger as the produced particles carry more and more of the initial particle’s center-of-mass momentum. Other effects, like the associated production of a kaon and a hyperon, can also contribute to an asymmetry in hyperon-antihyperon production [12].

As a byproduct of our charm program in Fermilab Experiment E769, we collected a large sample of Λ^0 and $\bar{\Lambda}^0$ hyperons which we have used to measure the particle-antiparticle production asymmetries reported here. Given E769’s variety of identified beam particles, we can study the production asymmetries as the content of valence quarks in the beam changes. This is the first such measurement in the central kinematical region (i.e., near $x_F = 0$) and with this variety of projectiles in a single experiment.

The asymmetry A can be defined as

$$A \equiv \frac{N_{\Lambda^0} - N_{\bar{\Lambda}^0}}{N_{\Lambda^0} + N_{\bar{\Lambda}^0}} \quad (1)$$

where N_{Λ^0} ($N_{\bar{\Lambda}^0}$) is the number of Λ^0 ($\bar{\Lambda}^0$) produced over the kinematic range of interest.

For all beam types, a positive asymmetry growing larger with increasingly negative x_F is expected, because Λ^0 (uds) shares two valence quarks with the target p (uud) or n (udd) while $\bar{\Lambda}^0$ ($\bar{u}\bar{d}\bar{s}$) shares none. For both the π^+ ($u\bar{d}$) and π^- ($\bar{u}d$) beams, an asymmetry close to zero is expected for $x_F > 0$, because Λ^0 and $\bar{\Lambda}^0$ each share one valence quark with the incident beam. For the K^+ ($u\bar{s}$) beam, a negative asymmetry which becomes more negative with increasing

x_F is expected for $x_F > 0$, because $\bar{\Lambda}^0$ shares the heaviest valence quark with the beam while Λ^0 shares only a light quark. The situation is reversed for the K^- ($\bar{u}s$) beam, where the asymmetry in the forward direction is expected to be positive and to become more positive with increasing x_F . For the p (uud) beam, a large positive asymmetry which grows even larger with increasing x_F is expected in the forward direction, because Λ^0 shares two valence quarks with beam proton while $\bar{\Lambda}^0$ shares none. Although measurements of Λ^0 and $\bar{\Lambda}^0$ production asymmetries have been made in several other experiments [1,13–17], no single experiment to date has been able to study the asymmetries and to compare them for all five beam types, π^- , π^+ , p , K^+ and K^- .

Experiment E769 recorded about 400×10^6 physics events from interactions of 250 GeV/ c hadron beams of both signs on a multifoil target of Be, Cu, Al and W. The negative beam consisted of 93% π^- , 5% K^- and 1.5% p^- , the positive beam of 61% π^+ , 4.4% K^+ , and 34% p . Event-by-event beam particle identification was accomplished through the use of a differential Čerenkov counter[18] and a transition radiation detector[19]. Pre-scaling of triggers was used to enhance the recorded sample of minority-beam-particle interactions.

The apparatus in Fermilab experiment E769 has been previously described (See [20–22] and references therein.) In this analysis we use the 11 silicon microstrip planes (1 - 30 cm downstream of the target), 35 drift chambers (150 - 1750 cm downstream of the target), 2 multiwire proportional chambers (130 cm, 180 cm downstream of the target), and 2 magnets (centered at 290 cm, 620 cm downstream of the target) for momentum measurement. The two threshold Čerenkov counters downstream of the target were not used and the electromagnetic and hadronic calorimeters were used only for on-line event selection. The trigger required that the total “transverse energy” (i.e., sum of the products of energy observed times the tangent of the angle from the target to each calorimeter segment) be at least 5.5 GeV. Most Λ^0 ’s decay before entering the drift chamber region, but downstream of the end of the silicon vertex detectors.

Throughout this paper, references to a particle should be taken to include its antiparticle except where explicitly stated otherwise. For historical reasons and current availability of data samples, the positive beam and negative beam samples come from rather different event selections. The positive beam Λ^0 ’s were reconstructed from Λ^0 ’s decaying upstream of the silicon vertex detector, while the negative beam sample comes from Λ^0 ’s decaying downstream and reconstructed using tracks which were not seen in the silicon vertex detector. In addition to the resulting differences in selection criteria, there are more Λ^0 data from the negative beam and consequently larger kinematic ranges are accessible.

All Λ^0 ’s were reconstructed using the $p\pi^-$ decay mode. Selection criteria were

chosen to maximize the signal significance using Monte Carlo simulation for the signal, and using side-band data for background projections. The ratio of proton to pion decay momenta was required to be larger than 3.0. For the positive beams (p , π^+ and K^+), proton and π^- tracks were required to make a vertex downstream of the last target, but upstream of the silicon detector, and have a distance of closest approach less than 0.02 cm. The resulting Λ^0 candidate track was then required to have an impact parameter relative to the interaction point of less than 0.006 cm. For the negative beams (π^- and K^-), the proton and π^- tracks were required to make a vertex downstream of the silicon detector, but upstream of the first analysis magnet. The tracks had to have a distance of closest approach less than 0.7 cm at the decay vertex, with no requirement on the impact parameter of the lambda candidate track.

The reconstructed mass distributions for each interval of x_F and p_T^2 were fit in the mass range from 1.101 to 1.127 GeV/c^2 using a binned maximum likelihood method with a Gaussian signal plus a linear background. All x_F and p_T^2 bin widths are much larger than the resolution of the variable binned. In the fit, the central reconstructed mass values and mass resolutions were fixed to values obtained from Monte Carlo simulation. Monte Carlo simulation studies demonstrated that $K_s^0 \rightarrow \pi^+\pi^-$ provided a flat background and produced a negligible effect on the fit numbers of Λ^0 's. The total reconstructed mass distributions are shown in Figs. 1 and 2. Table 1 shows the total numbers of Λ^0 and $\bar{\Lambda}^0$ from the fits shown.

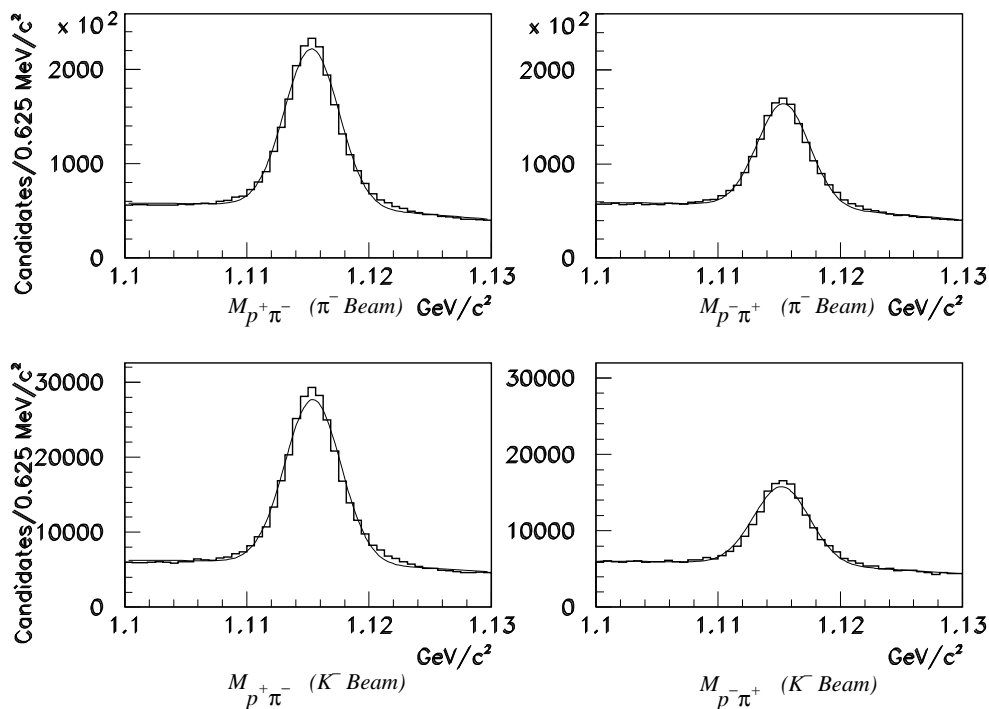


Fig. 1. Effective $p\pi$ mass distributions for the negative beams.

For each x_F and p_T^2 bin we compute an asymmetry, A , as defined in Equation

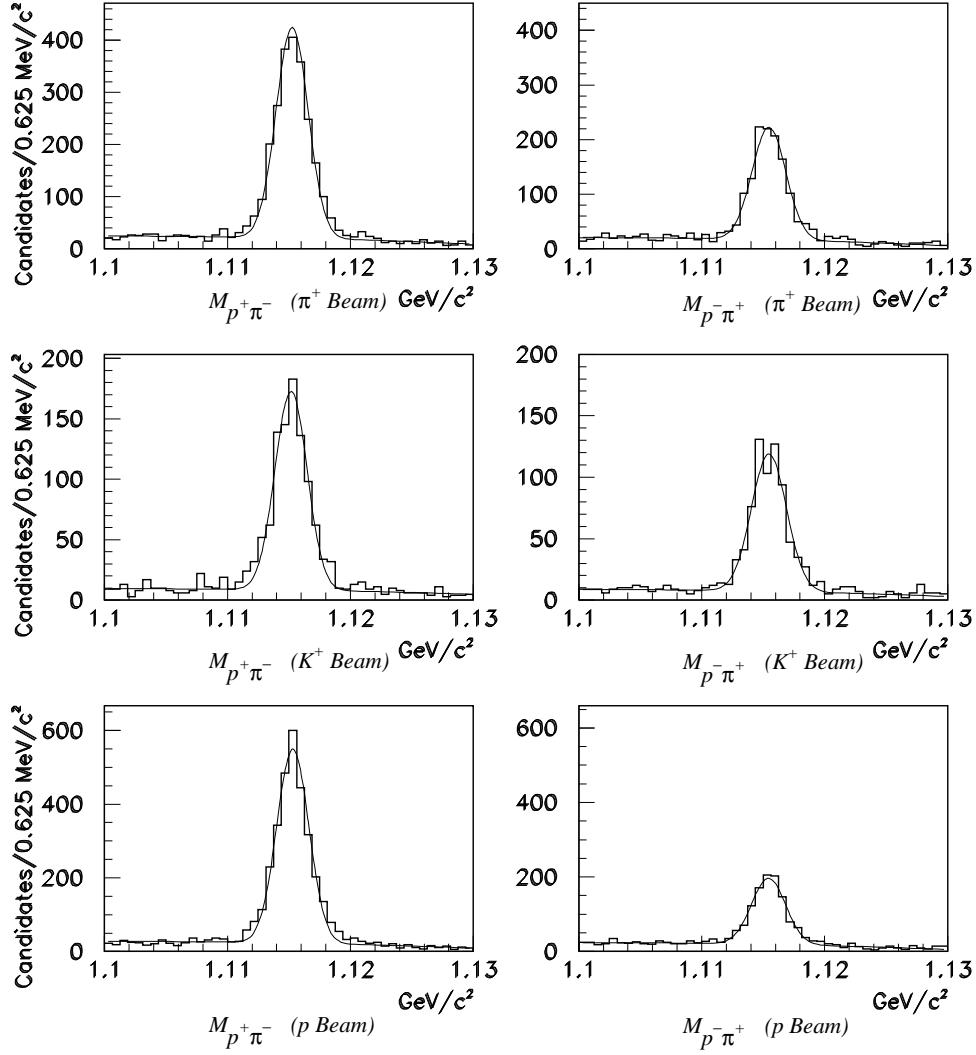


Fig. 2. Effective $p\pi$ mass distributions for the positive beams.

Beam	Λ^0	$\bar{\Lambda}^0$
π^+	$1,965 \pm 49$	$1,053 \pm 37$
π^-	$1,537,000 \pm 1,877$	$996,200 \pm 1,712$
K^+	845 ± 32	621 ± 28
K^-	$203,800 \pm 660$	$95,300 \pm 548$
p	$2,615 \pm 56$	919 ± 35

Table 1

Total number of Λ^0 and $\bar{\Lambda}^0$ observed for each beam. The errors are statistical as determined by the fits.

1. Values for the N 's were obtained from individual fits to the $p\pi$ mass plots for events selected to lie within each x_F and p_T^2 interval. For each beam type, the asymmetry $A(x_F)$ integrated over p_T^2 , and the asymmetry $A(p_T^2)$ integrated

over our range of x_F , are presented in Figs. 3 and 4. The results are also listed in Tables 2, 3, 4, and 5 along with statistical errors.

The experimental apparatus itself could create an apparent particle-antiparticle asymmetry if there were a difference in the detection efficiencies for Λ^0 and $\bar{\Lambda}^0$. Selection criteria for the particle and antiparticle samples were identical. However, geometrical acceptances and reconstruction efficiencies were not necessarily the same. To evaluate this potential effect, a large sample of simulated events was created using the PYTHIA/JETSET event generators [25,26]. These were passed through a detailed simulation of the E769 spectrometer to simulate “data” in digitized format, which was then processed through the same computer reconstruction code as that used for data from the experiment. Simulated event data were subjected to the same selection criteria as used for detector data. No difference was found between the acceptances and efficiencies for Λ^0 compared to $\bar{\Lambda}^0$ at a level significant with respect to the statistical errors.

We also looked for systematic effects from the other following sources:

- Event selection criteria;
- The minimum transverse energy in the calorimeters required in the on-line event selection;
- K_S contamination of the Λ^0 signal;
- Misidentification of beam particle types;
- Λ^0 from higher-mass hyperon decays;
- Mass fits (shape);

All seven sources, the relative efficiencies and the six others listed, were found to produce systematic effects that were negligible in each kinematic bin, both individually and in the ensemble, when compared to the statistical uncertainties.

The behavior of the asymmetries shown in Figs. 3 and 4 have leading particle effects where expected. A larger asymmetry is observed when there is a larger difference in the number of valence quarks in the Λ^0 or $\bar{\Lambda}^0$ in common with the target or the various beams. We [23] and others [2,24] have reported evidence for similar effects in the production of D^\pm mesons in the forward region ($x_F > 0$).

The PYTHIA **6.2** [27] model describes only some features of our results, and those only qualitatively, as can be seen in Fig. 3 and Fig. 4. This model predicts small values of asymmetry for $x_F = 0$ in contrast to our results which have large asymmetries in this region. This may be due to associated production of strange mesons and baryons (more $\Lambda^0 \bar{K}$ than $\bar{\Lambda}^0 K$). Leading particle effects play an increasingly important role as $|x_F|$ increases.

Our results for particle-antiparticle asymmetries are consistent with the results obtained by other experiments where similar data exists [1,13,28]. Our results can be described qualitatively in terms of the energy thresholds for the production of hyperons and antihyperons together with their associated particles and a model in which the recombination of valence quarks in the beam and target particles contributes to the hyperon and antihyperon production in an asymmetrical manner [29].

In summary, we report a precise, systematic study of the production asymmetries for Λ hyperons by various incident hadrons in a single experiment. The range of x_F covered allows the study of asymmetries in regions close to $x_F = 0$. Our results are consistent with other experiments where similar data exists and while models so far describe some features of our results, they do so only qualitatively.

We gratefully acknowledge the assistance of the staffs of Fermilab and of all the participating institutions. This research was supported by the Brazilian Conselho Nacional de Desenvolvimento Científico e Tecnológico, the U.S. National Science Foundation, the U.S. Department of Energy, and the National Research Council of Canada. Fermilab is operated by the Universities Research Association, Inc., under contract with the United States Department of Energy.

References

- [1] E. M. Aitala et al.(E791 Collaboration), Phys. Lett. B 496 (2000) 9.
- [2] E.M. Aitala et al. (E791 Collaboration), Phys. Lett. B 371 (1996) 157.
- [3] G.A. Alves et al. (E769 Collaboration), Phys. Rev. Lett. **72** (1994) 812 and **72** (1994) 1946.
- [4] M. Adamovich et al. (WA92 Collaboration), Nucl. Phys. **B 495** (1997) 3.
- [5] E.M. Aitala et al. (E791 Collaboration), Phys. Lett. B 411 (1997) 230.
- [6] L. G. Pondrom, Phys. Rept. 122 (1985) 57.
- [7] V.G. Kartvelishvili, A.K. Likhoded, and S.R. Slobospitskii, Sov. J. Nucl. Phys. **33** (1981) 434.
- [8] R.C. Hwa, Phys. Rev. **D 51** (1995) 85.
- [9] R. Vogt and S.J. Brodsky, Nucl. Phys. **B 478** (1996) 311.
- [10] B.W. Harris, J. Smith, and R. Vogt, Nucl. Phys. **B 461** (1996) 181.
- [11] G. Herrera and J. Magnin, Eur. Phys. J. **C 2** (1998) 477.

- [12] A. Capella, U. Sukhatme, C.I. Tan, and J. Tran Thanh Van, Phys. Rev. **D 36** (1987) 109.
- [13] S. Barlag et al. (ACCMOR Collaboration), Phys. Lett. B 325 (1994) 531.
- [14] S. Mikocki et al. (E580 Collaboration), Phys. Rev. **D 34** (1986) 42.
- [15] R.T. Edwards et al. (E415 Collaboration), Phys. Rev. **D 18** (1978) 76.
- [16] N.N. Biswas et al. (E002, E281, and E597 Collaborations), Nucl. Phys. **B 167** (1980) 41.
- [17] D. Bogert et al. (E234 Collaboration), Phys. Rev. **D 16** (1977) 2098.
- [18] M. Benot, J. Litt, and R. Meunier, Nucl. Instr. and Meth. 105 (1972) 431.
- [19] D. Errede et al., Nucl. Instr. and Meth. Phys. Res., Sect **A 309** (1991) 386.
- [20] J. Appel, Annu. Rev. Nucl. Part. Sci. **42** (1992) 367.
- [21] C. Gay and S. Bracker, IEEE Trans. Nucl. Sci. **34** (1987) 870.
- [22] G. A. Alves et al. (E769 Collaboration), Phys. Rev. Lett. **69** (1992) 3147.
- [23] G.A. Alves et al. (E769 Collaboration), Phys. Rev. Lett. **77** (1996) 2388; G.A. Alves et al. (E769 Collaboration), Phys. Rev. Lett. **81** (1998) 1537.
- [24] M. Adamovich et al. (WA82 Collaboration), Phys. Lett. B 305 (1993) 402.
- [25] T. Sjöstrand, PYTHIA 5.7 and JETSET 7.4. Physics and Manual, CERN-TH-7112/93 (1993) hep-ph/9508391.
- [26] H.U. Bengtsson and T. Sjöstrand, Comput. Phys. Commun. **46** (1987) 43.
- [27] T. Sjöstrand, L. Lönnblad, S. Mrenna, “PYTHIA 6.2”, hep-ph/0108264, (2001).
- [28] S. Barlag et al. (ACCMOR Collaboration), Phys. Lett. B 233 (1989) 522.
- [29] J.C. Anjos, J. Magnin, F.R.A. Simão, and J. Solano, Proceedings of II Silafae, AIP Conf. Proc. 444 (1998) 540, hep-ph/9806396.

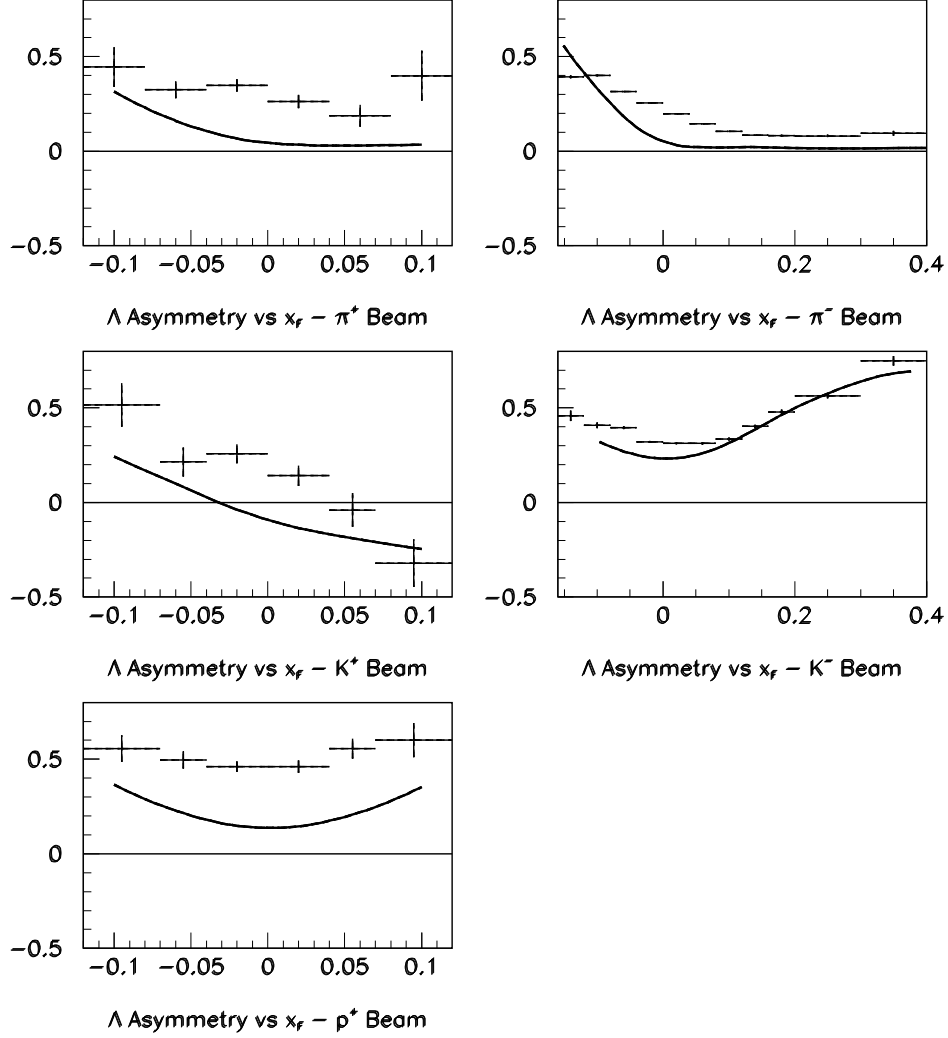


Fig. 3. Λ^0 production asymmetries vs x_F for various incident beams. The errors shown are statistical, with systematic errors being negligible. The curves are predictions of the PYTHIA 6.2 model.

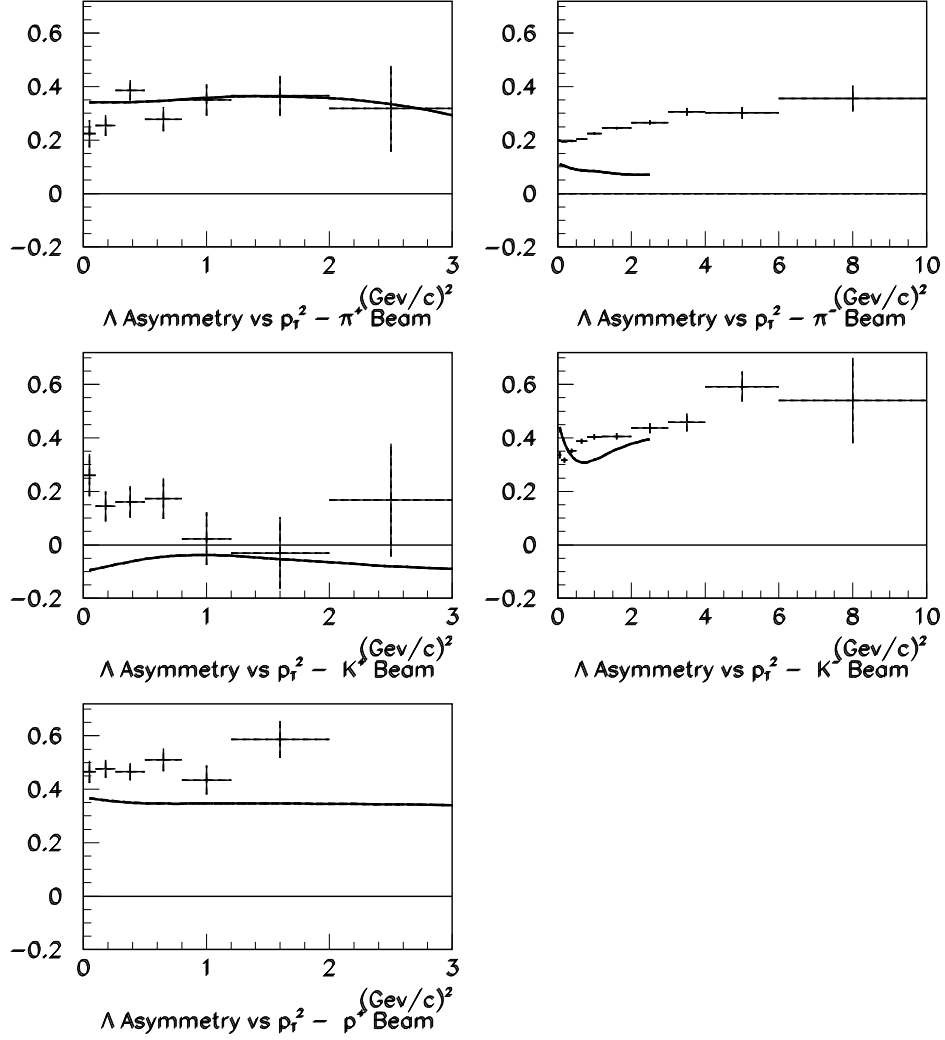


Fig. 4. Λ^0 production asymmetries vs p_T^2 for various incident beams. The errors shown are statistical, with systematic errors being negligible. The curves are predictions of the PYTHIA 6.2 model. The prediction of PYTHIA is limited to the range of p_T^2 shown.

Beam	x_F Region	Production Asymmetry
π^+	$-0.12 \leq x_F < -0.08$	0.446 ± 0.105
	$-0.08 \leq x_F < -0.04$	0.325 ± 0.045
	$-0.04 \leq x_F < 0.00$	0.349 ± 0.033
	$0.00 \leq x_F < +0.04$	0.263 ± 0.036
	$+0.04 \leq x_F < +0.08$	0.188 ± 0.058
	$+0.08 \leq x_F \leq +0.12$	0.399 ± 0.132
K^+	$-0.12 \leq x_F < -0.08$	0.516 ± 0.116
	$-0.08 \leq x_F < -0.04$	0.214 ± 0.076
	$-0.04 \leq x_F < 0.00$	0.258 ± 0.050
	$0.00 \leq x_F < +0.04$	0.142 ± 0.054
	$+0.04 \leq x_F < +0.08$	-0.040 ± 0.090
	$+0.08 \leq x_F \leq +0.12$	-0.321 ± 0.125
p^+	$-0.12 \leq x_F < -0.08$	0.556 ± 0.071
	$-0.08 \leq x_F < -0.04$	0.497 ± 0.046
	$-0.04 \leq x_F < 0.00$	0.461 ± 0.027
	$0.00 \leq x_F < +0.04$	0.461 ± 0.032
	$+0.04 \leq x_F < +0.08$	0.556 ± 0.053
	$+0.08 \leq x_F \leq +0.12$	0.601 ± 0.089

Table 2

Λ^0 production asymmetries vs x_F for positive beams. The errors shown are statistical, with systematic errors being negligible.

Beam	p_T^2 Region	Production Asymmetry
π^+	$0.00 < p_T^2 \leq 0.10$	0.224 ± 0.051
	$0.10 < p_T^2 \leq 0.26$	0.255 ± 0.039
	$0.26 < p_T^2 \leq 0.50$	0.387 ± 0.039
	$0.50 < p_T^2 \leq 0.80$	0.279 ± 0.046
	$0.80 < p_T^2 \leq 1.20$	0.350 ± 0.059
	$1.20 < p_T^2 \leq 2.00$	0.367 ± 0.074
	$2.00 < p_T^2 \leq 3.00$	0.318 ± 0.161
K^+	$0.00 < p_T^2 \leq 0.10$	0.261 ± 0.079
	$0.10 < p_T^2 \leq 0.26$	0.144 ± 0.056
	$0.26 < p_T^2 \leq 0.50$	0.160 ± 0.059
	$0.50 < p_T^2 \leq 0.80$	0.173 ± 0.077
	$0.80 < p_T^2 \leq 1.20$	0.023 ± 0.099
	$1.20 < p_T^2 \leq 2.00$	-0.031 ± 0.134
	$2.00 < p_T^2 \leq 3.00$	0.168 ± 0.211
p^+	$0.00 < p_T^2 \leq 0.10$	0.465 ± 0.042
	$0.10 < p_T^2 \leq 0.26$	0.476 ± 0.034
	$0.26 < p_T^2 \leq 0.50$	0.466 ± 0.033
	$0.50 < p_T^2 \leq 0.80$	0.509 ± 0.043
	$0.80 < p_T^2 \leq 1.20$	0.434 ± 0.054
	$1.20 < p_T^2 \leq 2.00$	0.586 ± 0.069
	$2.00 < p_T^2 \leq 3.00$	0.603 ± 0.144

Table 3

Λ^0 production asymmetries vs p_T^2 for positive beams. The errors shown are statistical, with systematic errors being negligible.

Beam	x_F region	Production Asymmetry
π^-	$-0.16 \leq x_F < -0.12$	0.393 ± 0.009
	$-0.12 \leq x_F < -0.08$	0.400 ± 0.005
	$-0.08 \leq x_F < -0.04$	0.316 ± 0.003
	$-0.04 \leq x_F < 0.00$	0.256 ± 0.002
	$0.00 \leq x_F < +0.04$	0.197 ± 0.002
	$+0.04 \leq x_F < +0.08$	0.146 ± 0.002
	$+0.08 \leq x_F < +0.12$	0.105 ± 0.002
	$+0.12 \leq x_F < +0.16$	0.085 ± 0.003
	$+0.16 \leq x_F < +0.20$	0.083 ± 0.005
	$+0.20 \leq x_F < +0.30$	0.081 ± 0.005
	$+0.30 \leq x_F \leq +0.40$	0.095 ± 0.013
K^-	$-0.16 \leq x_F < -0.12$	0.458 ± 0.027
	$-0.12 \leq x_F < -0.08$	0.408 ± 0.014
	$-0.08 \leq x_F < -0.04$	0.395 ± 0.007
	$-0.04 \leq x_F < 0.00$	0.320 ± 0.006
	$0.00 \leq x_F < +0.04$	0.314 ± 0.005
	$+0.04 \leq x_F < +0.08$	0.312 ± 0.006
	$+0.08 \leq x_F < +0.12$	0.335 ± 0.007
	$+0.12 \leq x_F < +0.16$	0.402 ± 0.009
	$+0.16 \leq x_F < +0.20$	0.479 ± 0.012
	$+0.20 \leq x_F < +0.30$	0.563 ± 0.011
	$+0.30 \leq x_F \leq +0.40$	0.749 ± 0.025

Table 4
 Λ^0 production asymmetries vs x_F for negative beams. The errors shown are statistical, with systematic errors being negligible.

Beam	p_T^2 Region	Production Asymmetry
π^-	$0.00 < p_T^2 \leq 0.10$	0.198 ± 0.004
	$0.10 < p_T^2 \leq 0.26$	0.195 ± 0.003
	$0.26 < p_T^2 \leq 0.50$	0.196 ± 0.003
	$0.50 < p_T^2 \leq 0.80$	0.204 ± 0.003
	$0.80 < p_T^2 \leq 1.20$	0.225 ± 0.004
	$1.20 < p_T^2 \leq 2.00$	0.245 ± 0.005
	$2.00 < p_T^2 \leq 3.00$	0.266 ± 0.008
	$3.00 < p_T^2 \leq 4.00$	0.306 ± 0.014
	$4.00 < p_T^2 \leq 6.00$	0.302 ± 0.022
	$6.00 < p_T^2 \leq 10.0$	0.356 ± 0.048
K^-	$0.00 < p_T^2 \leq 0.10$	0.336 ± 0.012
	$0.10 < p_T^2 \leq 0.26$	0.317 ± 0.009
	$0.26 < p_T^2 \leq 0.50$	0.352 ± 0.008
	$0.50 < p_T^2 \leq 0.80$	0.388 ± 0.009
	$0.80 < p_T^2 \leq 1.20$	0.404 ± 0.010
	$1.20 < p_T^2 \leq 2.00$	0.406 ± 0.012
	$2.00 < p_T^2 \leq 3.00$	0.436 ± 0.019
	$3.00 < p_T^2 \leq 4.00$	0.459 ± 0.033
	$4.00 < p_T^2 \leq 6.00$	0.592 ± 0.055
	$6.00 < p_T^2 \leq 10.0$	0.540 ± 0.160

Table 5

Λ^0 production asymmetries vs p_T^2 for negative beams. The errors shown are statistical, with systematic errors being negligible.